A pharmacophore model for NK2 antagonist comprising compounds from several structurally diverse classes

Anders Poulsen[a,b], Tommy Liljefors[a*], Klaus Gundertofte[b] and Berith Bjørnholm[b]

[a]*Department of Medicinal Chemistry, The Royal Danish School of Pharmacy, 2 Universitetsparken, DK-2100 Copenhagen, Denmark*
[b]*H. Lundbeck A/S, 9 Ottiliavej, DK-2500 Copenhagen-Valby, Denmark*

Summary

A neurokinin 2 (NK2) antagonist pharmacophore model has been developed on the basis of five non-peptide antagonists from several structurally diverse classes. To evaluate the pharmacophore model, another 20 antagonists were fitted to the model. By use of exhaustive conformational analysis (MMFFs force field and the GB/SA hydration model) and least-squares molecular superimposition studies, 23 of the 25 antagonists were fitted to the model in a low energy conformation with a low RMS value. The pharmacophore model is described by four pharmacophore elements: Three hydrophobic groups and a hydrogen bond donor represented as a vector. The hydrophobic groups are generally aromatic rings, but this is not a requirement. The antagonists bind in an extended conformation with two aromatic rings in a parallel displaced and tilted conformation. The model was able to explain the enantioselectivity of SR48968 and GR159897.

Introduction

The tachykinins or neurokinins (NKs) Substance P (SP), neurokinin A (NKA), and neurokinin B (NKB) are regulatory peptides that play an important role in immune responses and as neurotransmitters and neuromodulators. The three peptides, SP, NKA and NKB bind to the neurokinin (NK) receptors NK1, NK2 and NK3 with affinities in the respective order [1]. NK receptors are distributed in the central nervous system (CNS), as well as in peripheral tissues, and belong to the superfamily of G-protein coupled receptors (GPCRs). As is the case for all GPCRs, except rhodopsin, NK receptors have not yet been crystallised, therefore no experimental structures are available.

NKs are involved in a number of pathological conditions, including psychiatric diseases like anxiety [2], depression [3], schizophrenia [4], neurodegradation [4], airways diseases like asthma [5] as well as numerous other diseases including pain [6], emesis [7], arthritis [8], etc. For that reason, NK receptors are of great interest as targets for the treatment of these diseases.

Since the discovery of the first non-peptide NK1 antagonist CP96345 [9], numerous NK1, NK2 and NK3 antagonists belonging to different structural classes have been published [10, 11]. Most of these compounds contain at least two aromatic ring systems connected by a linker holding a hydrogen bond acceptor. We define the part of the NK antagonists containing the two aromatic rings as the head of the molecules, and the rest is defined as the tail (Figure 1). The major difference between the NK1 and NK2 antagonists is that only the head fragment is required to obtain high NK1 (nM range) affinity while also the tail is required for NK2 affinity. However, addition
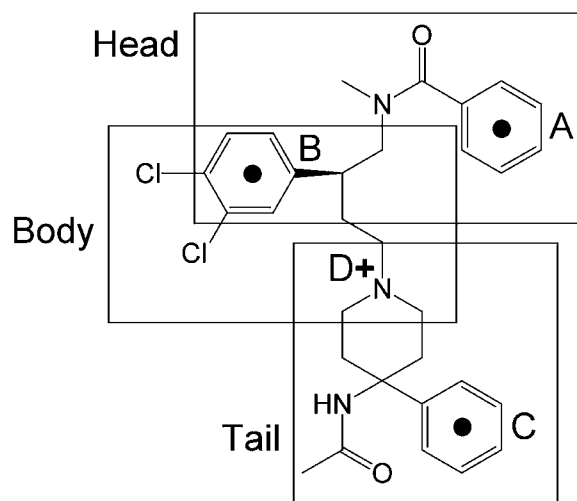
Corresponding author: Prof. Tommy Liljefors, Department of Medicinal Chemistry, The Royal Danish School of Pharmacy, 2 Universitetsparken, DK-2100 Copenhagen, Denmark; Tel.: +45 35 30 65 05; Fax: +45 35 30 60 40; e-mail: tl@dfh.dk

of a tail also enhances affinity of most NK1 antagonists. Figure 2 shows the structure of the selective NK1 antagonist CP99994 [12].

A number of NK1 pharmacophore models have been published [13–18], and there is a fair agreement on the definition of the pharmacophore elements. Apart from a few studies [13, 14], there is consensus about an arrangement with the two aromatic ring systems in a tilted arrangement (Figure 2) [19]. We present an NK2 pharmacophore model that contains the same aromatic ring systems as the published NK1 pharmacophore models, but in a different arrangement. In this model, the aromatic groups are parallel displaced and tilted [20]. These results agree with previously published NK1, NK2, and μ-opioid receptor model studies. Thus, in a study of the dual NK1 and NK2 antagonist MDL103,392 (a close analogue of compound **4** in Figure 3) by 7-TM receptor modelling, Greenfeder et al. [21] proposed the compound to bind to the NK1 receptor in a conformation represented by the NK1 pharmacophore model in Figure 2. The ligand is predicted to bind to the NK2 receptor in an extended conformation with the two aromatic rings in a parallel displaced and tilted orientation. (Note, that the docked structure displayed in the paper is not MDL103,392). Blaney et al. [22] docked dual NK2 and NK3 antagonists of the 2-phenylquinoline class (analogues of compound **18** in Figure 3) into 7-TM models of the NK2, NK3 and μ-opioid receptors. These compounds are predicted to bind to the NK2 receptor in an extended conformation with two aromatic

ring systems in an arrangement similar to a parallel displaced and tilted orientation.

Computational methods

Conformational search and force fields

The molecules were built using MacroModel 7.0 [23]. The basic amines were protonated as in an aqueous solution at physiological pH. The conformational space was then searched using the Monte Carlo (MCMM) method [24]. All heavy atoms and hydrogens on heteroatoms were superimposed in the test for duplicate conformations. All rotatable single bonds were included in the conformational search. All flexible rings were ring-opened and quaternary carbon and nitrogen atoms were allowed to invert. The search was continued until the lowest energy conformations were found at least five times. The energy minimisations were carried out with the truncated Newton conjugate gradient (TNCG) algorithm and the MMFF94s [25, 26] force field as implemented in MacroModel. Default parameters was used. For compounds for which no low energy conformation that fitted the model could be found, further conformational searches by this standard procedure using the AMBER*, MM3* and MM2* force fields as implemented in MacroModel were performed.

Solvation model

The conformational searches were done for aqueous solution with the Generalised Born/Solvent Accessible surface (GB/SA) continuum solvation model [27, 28] as implemented in MacroModel. Default parameters were applied, except that van der Waals and electrostatic cut-offs were set to 100 Å. This means effectively no cut-offs on van der Waals and electrostatic forces.

Calculation of the conformational energy penalty

The conformational energy penalty for the putative bioactive conformation of each ligand was calculated by subtracting the internal (steric) energy of the preferred conformation in aqueous solution (i.e. the energy of the global minimum in solution excluding the hydration energy) from the calculated energy of the putative bioactive conformation [29]. Since the conformational ensemble was represented by only the global minimum, entropy effects have not been taken into account. For flexible molecules this leads to an
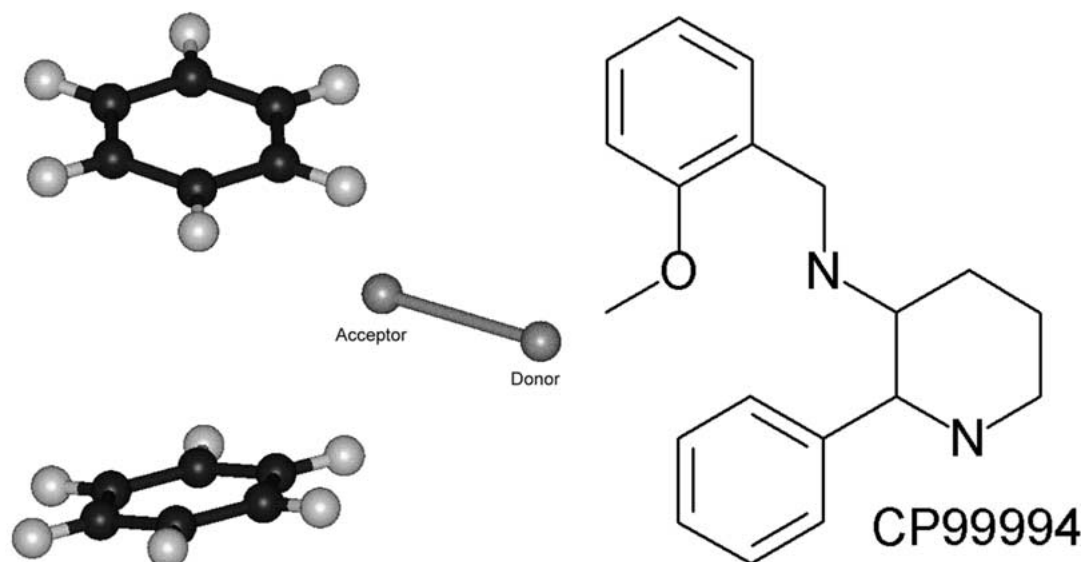
Figure 2. Left: The generally accepted NK1 pharmacophore model. Two aromatic rings in a tilted arrangement with a hydrogen bond acceptor (represented as a vector) in the arm connecting the two rings. To the right is shown the selective NK1 antagonist CP99994 [12].

underestimation of the energy penalty. A limit of 3 kcal/mol (12.6 kJ/mol) for acceptable energy penalties was imposed as recommended by Boström et al. [29].

Superimposition studies

Three aromatic rings and a hydrogen bond donor (in most cases the protonated nitrogen atom of an amine) were chosen as pharmacophore elements. For each of the aromatic rings, centroids were constructed. A putative hydrogen bonding site point was represented by a dummy atom 2.8 Å from the nitrogen in the direction of the nitrogen-hydrogen bond. The dummy atom was not used as a fitting point, but used to evaluate the direction of the hydrogen bond donor-acceptor interaction. The centroids and the nitrogen atom of the hydrogen bond donor were used for superimposing the ligands. Least-squares rigid body molecular superimpositions were performed using Macromodel. The superimposition was evaluated in terms of RMS values of the fitting points. An RMS value of 0.6 Å has been used as a soft indicator to determine whether a fit is acceptable or not. The aromatic pharmacophore elements were fitted in a coplanar orientation if energetically possible. The RMS values do not give any measure of this coplanarity since only the centroids are superimposed.

Flo99 flexible superimposition search

The automatic fitting program Flo99 [30, 31] was used to check if all possible fits had been taken into account during the manual fitting. Structures were built and imported from MacroModel into program Flo99. Only two structures were fitted at a time. Either one structure was used as a template or both structures were kept flexible. The output from Flo99 was exported back into MacroModel where each structure was relaxed by using flat bottom cartesian constraints with a half width of 0.2 Å and the default restraining force constant of 500 kJ/mol*Å^2. The conformational energy was calculated using the MMFF94s force field [29].

pKa calculations

In order to identify the most basic nitrogen for compounds containing more than one basic nitrogen, pK_a were calculated for the most basic nitrogen by use of the program MolSurf 99/1 [32]. MolSurf requires a Spartan [33] archive file as input. Each of the unprotonated putative bioactive conformations was imported into Spartan for a full AM1 geometry optimisation followed by a single point HF calculation with the 3-21G* basis set. Default settings were used.
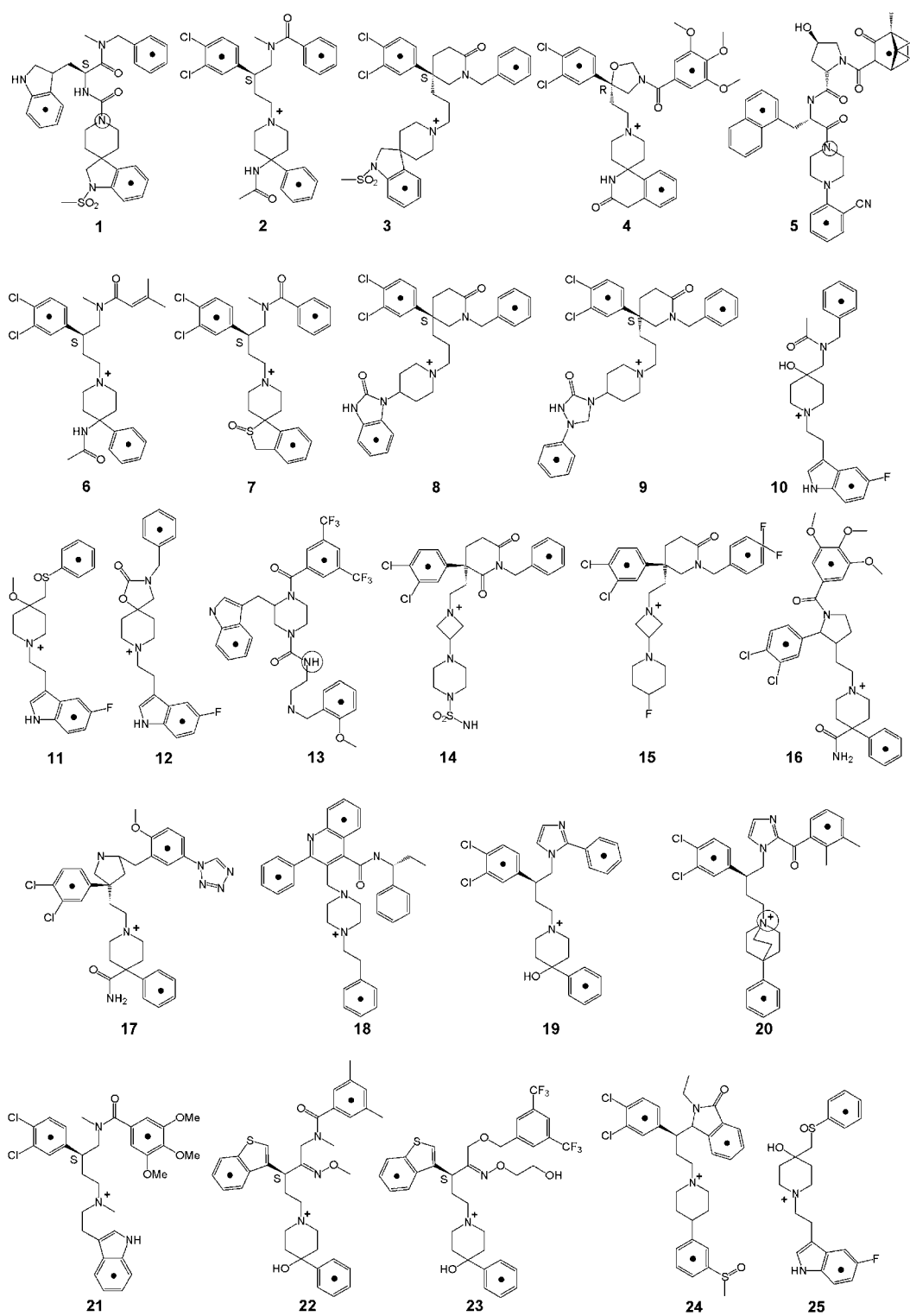
276

Figure 3. Compounds **1–5** were used to derive the pharmacophore model. The remaining compounds are used for validating the model. Centroids and '+' mark the selected pharmacophore elements. A circle marks a fitting point in compounds without basic nitrogen. Data and references are given in Table 1.

Table 1. Data of compounds fitted to the pharmacophore model. Calculated conformational energy penalties for putative bioactive conformations. pK_a values of the amine pharmacophore element.

Compound	NK2 Activity nM		Energy kJ/mol		RMS Å		pK_a
	IC_{50}	K_i	Equatorial	Axial	Equatorial	Axial	
1 [35]	24		1.4	10.4	0.61	0.69	–
(S)-**2** (S-SR48968) [36]		0.5	−2.3	3.6	Template	Template	9.1
(R)-**2** (R-SR48968) [36]		945	17.0	21.1	0.37	0.30	9.1
3 [37]	2.2		2.9	2.7	0.85	0.88	8.9
4 [38]	3.0		−7.6	−3.5	0.19	0.31	8.9
5 (DE4445939a1) [39]	19		2.6	8.1	0.27	0.41	–
6 [40]	11		−63.4	−75.2	0.25	0.42	9.1
7 (YM38336) [41]	8.9		6.4	39.4	0.11	0.36	9.1
8 [37]	6.4		35.2	10.2	0.78	1.44	9.0
9 [37]	2.5		4.0	16.3	0.42	0.67	8.9
10 [42]		1.6	5.4	2.9	0.31	0.53	9.2
(R)-**11** (R-GR159897) [43]		0.1	−0.2	−10.6	0.42	0.61	9.1
(S)-**11** (S-GR159897) [43]	N.A.	N.A.	6.2	12.1	0.39	0.58	9.1
12 [42]		1.3	1.2	−0.5	0.40	0.43	9.1
13 (EP899270a1) [44]	60		118.9	28.4	0.67	0.51	10.1
14 (EP791592a2) [45]	0.5		31.8	73.0	0.27	0.38	7.6
15 (WO9727185a1) [46]		0.6	6.5	6.5	0.40	0.57	8.3
16 (US5824690a) [47]	7.93		−8.5	4.4	0.41	0.52	9.0
17 (WO9827086a1) [48]	16.3		12.4	29.9	0.47	0.47	9.0
18 (WO9852942a1) [49]	0.9	0.9	10.0	15.2	0.90	0.60	6.3
19 (EP739891a2) [50]		23	9.8	21.6	0.63	0.70	9.0
20 (WO9857972a1) [51]	4		−0.9	0.5	0.46	0.85	–
21 [52]		33	7.1	1.8	0.18	0.50	10.1
22 (US5688960a) [53]		4.5	3.5	6.5	0.90	0.77	9.2
23 [54]		23	−4.9	1.1	0.31	0.32	–
24 (ZD7944) [55]	8.9		−3.6	−0.5	0.77		9.0
(R)-**25** [43]		0.3	10.3	16.9	0.56	0.63	9.1
(S)-**25** [43]		7.9	−37.0	−31.9	0.43	0.50	9.1

N.A. = Not available

Results and discussion

Construction of the pharmacophore model

The NK2 antagonists used to derive and evaluate the pharmacophore model are shown in Figure 3. The set was chosen on the basis of high NK2 receptor affinity and structural diversity. Selective NK2 as well as dual NK1 and NK2 antagonists are included in the set. Affinity data and references for the compounds are given in Table 1. Most of the compounds are highly flexible and, in order to derive the model, the molecules were cut into three fragments as defined in Figure 1. The fragments overlap partly, which means that the fragments can finally be assembled in an unambiguous way. Three to four pharmacophore elements were defined for each compound. The aromatic pharmacophore elements are marked in Figure 3 with a centroid and the basic nitrogens with a '+'. Compounds **1–5** were used to derive the pharmacophore model. For these compounds, each of the defined fragments contains two pharmacophore elements (Figures 1 and 3). The fragments were used to derive three sub-pharmacophores, which were assembled into the final NK2 pharmacophore model.

An exhaustive conformational analysis of the head fragments of compounds **3** and **4** were performed (Figure 4) in order to find the 3D arrangement of the pharmacophore elements A and B (Figure 1). These structures were selected because of their relative rigid-
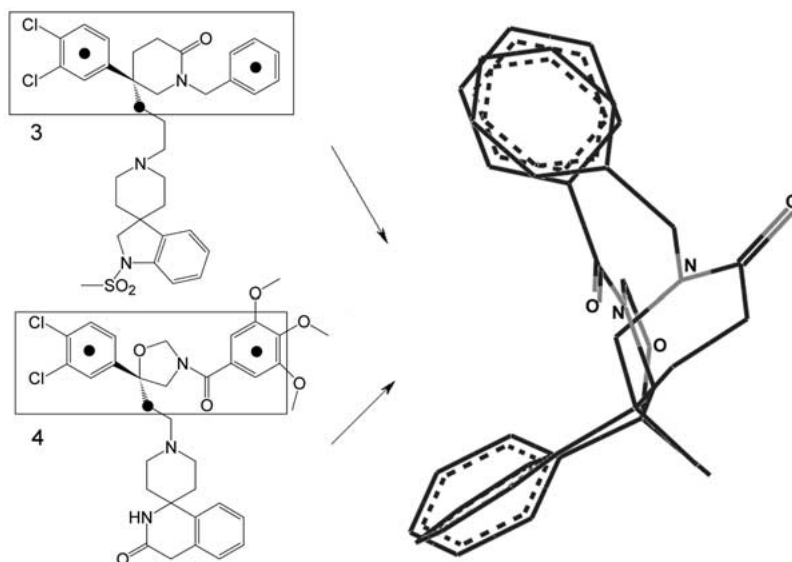
Figure 4. Superimposition of the head fragments of compounds **3** and **4**. The two fragments could only be superimposed well in the conformations shown. Solid dots mark the fitting points. RMS = 0.32 Å.

ity. Four conformations of the fragment of compound **4** were found within 50 kJ/mol of the global energy minimum, and 16 conformations of the fragment of compound **3**. When removing the tail fragments a methyl group is formed on the quarternary atoms of the aliphatic rings. Since the spiropiperidine tails of compounds **3** and **4** should occupy the same area, the carbon atoms of the methyl groups were used as fitting points together with the centroids of the aromatic rings (Figure 4). Only one reasonable superimposition of the two fragments could be obtained. Flexible fitting of the fragments using the semi-automatic program Flo99 gave the same result as that obtained by rigid body least squares superimposition.

To derive the tail sub-pharmacophore, conformational searches of the tail fragments of compounds **3** and **4** were performed (Figure 5). Four conformations of the fragment from compound **4** and 21 conformations of the fragment from compound **3** were found within 50 kJ/mol of the global energy minimum. The fragments could be superimposed in two different ways as shown in Figure 5, one in which the aromatic ring is in an equatorial position on the piperidine ring and one in which it is axial. The two different conformations have similar conformational energies. The aromatic rings and the piperidine rings superimpose very well in both conformations with RMS values below 0.1 Å. Note that the protonated amino groups have their hydrogens pointing in the same direction. By use

Table 2. Cartesian coordinates (Å) for the pharmacophore elements A–D.

Pharmacophore element	x	y	z
A	−1.906	8.804	−1.256
B	−4.474	2.919	0.919
C equatorial	3.219	−4.749	0.374
C axial	−1.468	−4.573	−0.340
D donor	0.000	0.000	0.000
D acceptor	2.462	1.317	0.214

of Flo99, the same superimpositions were obtained, and the axial and the equatorial conformations were found to have similar energies (data not shown).

Compounds **1** and **5** contain the most rigid 'body' fragments. These fragments were fitted by the use of Flo99. Two reasonable superimpositions were found as shown in Figure 6. Both of these superimpositions overlay very well with the linker part of the global energy minimum conformation of the (S)-enantiomer of compound **2**. An identical linker fragment is found in several of the molecules. This conformation of the body fragment is also found in the global energy minima conformations of compounds **4, 6, 19–21** and **24** and was chosen as the body sub-pharmacophore.

Finally, the three sub-pharmacophores were connected. This produced two pharmacophore models,
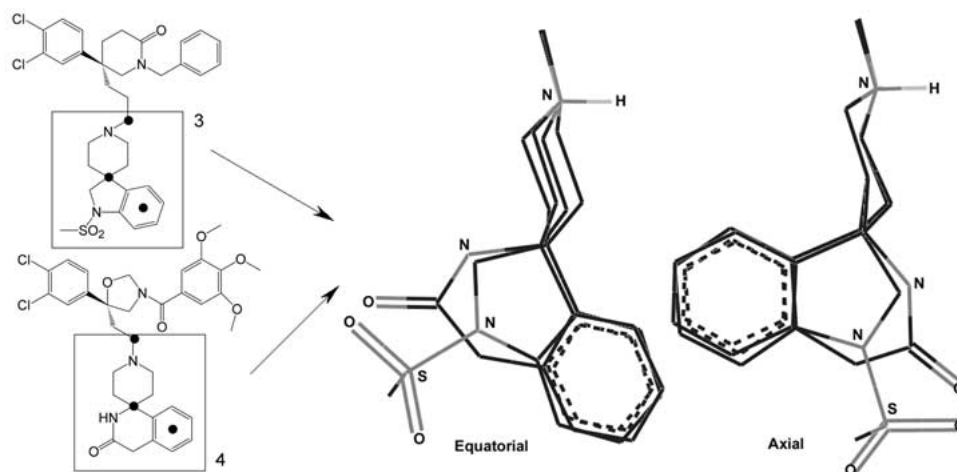
Figure 5. Superimposition of the tail fragments of structures **3** and **4**. Both an equatorial (left) and an axial conformation (right) were found. Energetically, there was no difference between the two conformations. Solid dots mark the fitting points. RMS = 0.08 (Equatorial), RMS = 0.07 (Axial).
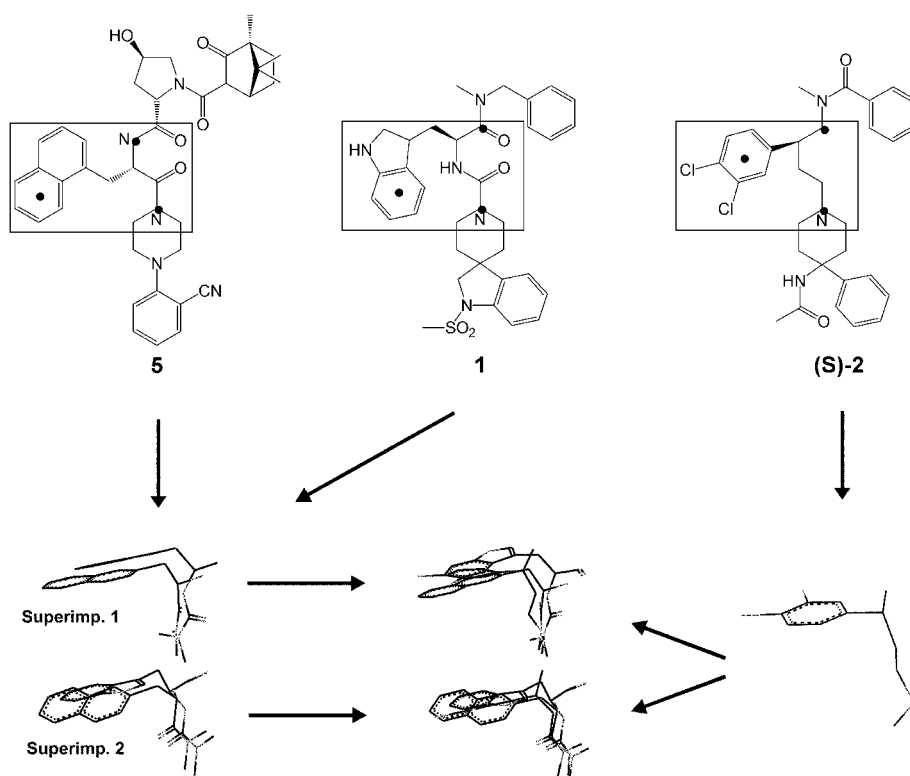

Figure 6. Left: Superimposition of the body fragments of structures **1** and **5**. Center: Superimposition of the body fragment from the global minimum of **(S)-2** onto **1** and **5**. Right: The body fragment of **(S)-2** was chosen as template. Solid dots mark the fitting points.

one in which the pharmacophore element C is in an equatorial position on the piperidine ring and one in which it is axial (Figure 7). It was found that two low energy minima of compound (S)-**2** superimpose very well onto all pharmacophore elements in each of the two pharmacophore models. Consequently, these conformations of compound (S)-**2** were used as templates on which all other compounds were superimposed (Figure 7). Cartesian coordinates for the derived pharmacophore elements A–D are given in Table 2.

Pharmacophore elements

Two or three hydrophobic groups are found in all NK2 antagonists (pharmacophore elements A, B and C, Figure 7). A basic amino group is also present in most structures (pharmacophore element D, Figure 7). The hydrophobic groups are marked in Figure 3 by centroids, and the basic nitrogen is marked with a positive charge. The pharmacophore element labelled B (Figure 7) is found to be an aromatic ring in all structures except compounds **10 – 12** and **25**. These compounds have electronegative groups in this area. Compounds **10** and **25** have a hydroxy group, compound **11** a methoxy group and compound **12** a carbonyl group. The pharmacophore element A need not be aromatic rings but can be aliphatic hydrophobes as is the case for compounds **5** and **6**. In compounds **14** and **15**, the aromatic pharmacophore element C is lacking. The basic amino group should be protonated at physiological pH as confirmed by pK_a calculations using MolSurf (Table 1). In all compounds having pharmacophore element D, this nitrogen always had the highest pKa value. If protonated, the amine can only act as a hydrogen bond donor, and the donor receptor interaction is represented as a vector of length 2.8 Å pointing in the direction of the nitrogen-hydrogen bond. The basic nitrogen is exchanged for a urea NH group in compounds **1** and **13**, an amide nitrogen in compound **5** and a quarternary nitrogen in compound **20**. It is known that a quarternary nitrogen can replace a basic amine as a pharmacophore element as previously described for e.g. muscarinic agonists [34].

Solvation energies

All the compounds, except **1, 5** and **22**, were found to have a solvation energy between −253 to −377 kJ/mol as calculated by using the GB/SA hydration model. Compounds **1** and **5** have a solvation energy of −163 kJ/mol and −187 kJ/mol respectively. These compounds do not contain a protonated nitrogen in the piperidine or piperazine ring. Since compounds **1** and **5** are lacking this hydrogen bond donor pharmacophore element, one would expect the compounds to have a low binding affinity for the NK2 receptor. This is, however, not the case (Table 1). Since the energy penalty for desolvation is much lower for these compounds, we suggest that the favourable desolvation energy make up for the loss of the pharmacophore element. Compound **13** has a protonated nitrogen, but according to our model, it is the urea group that holds the hydrogen bond donor pharmacophore element. The solvation energy is highly negative (−346.5 kJ/mol) but the interaction energy of the urea group with the receptor is lower than for a basic nitrogen. Therefore, one would expect the ligand to have a lower affinity for the receptor than ligands with a basic amine hydrogen bond donor. This can explain that compound **13** have an IC_{50} of 60 nM, whereas most of the other ligands studied have an affinity below 10 nM.

Evaluation of the model

It was possible to fit most compounds onto the 'axial' as well as 'equatorial' pharmacophore model (Figure 7) in a low energy conformation and with low RMS values. In contrast to the compounds used to derive the tail part of the pharmacophore model (compounds **3** and **4**), the conformations of the evaluation set fitted to the 'equatorial' model are energetically favoured over the conformations fitted to the 'axial' model (Table 1). This was expected since bulky substituents on cyclohexane prefer an equatorial conformation. There are no conclusive facts that can determine whether the 'equatorial' or 'axial' pharmacophore model represents the conformation that binds to the receptor. However, a number of observations lead us to conclude that it is the conformations fitted to the equatorial model that bind to the receptor. The average conformational energy penalty is higher for the conformations fitted to the 'axial' model. The hydrogen bonding groups of the tail fragment of some compounds only fall into the same area in the conformations fitted to the 'equatorial' model (e.g. **2, 7** and **17**). The aromatic pharmacophore element C of the spiro compounds **1, 3, 4** and **7** could be fitted to the 'equatorial' model in a coplanar orientation but not to the 'axial' model.

Some of the ligands have RMS values above 0.6 Å (Table 1). In compound **1**, pharmacophore element B (an indole ring) superimposes onto the template in
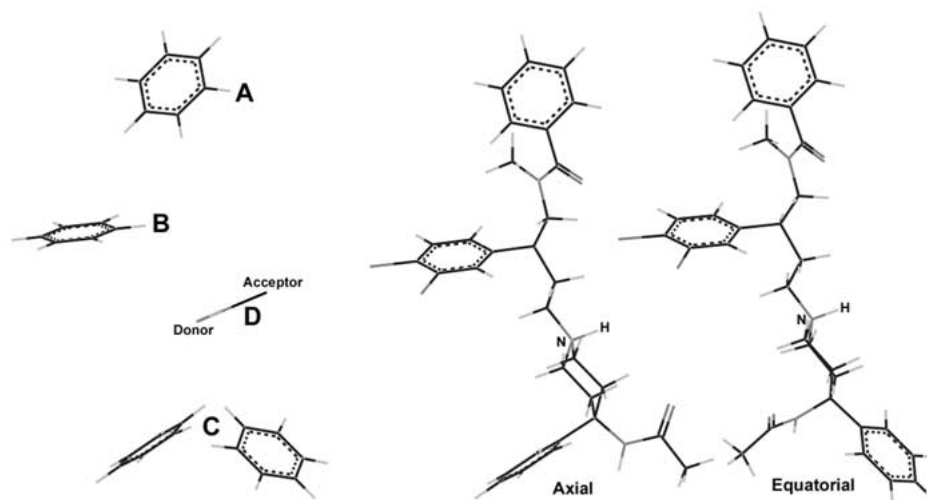
Figure 7. The final pharmacophore model. Left: Arrangement of pharmacophore elements. Element C can be in an axial or equatorial conformation. We propose that the equatorial conformation is most likely to be the bioactive conformation. Center and right: The putative bioactive conformations of **(S)-2** with pharmacophore element C axial (center) and equatorial (right). These two conformations were chosen as templates for fitting of the validation set.

a coplanar orientation, but the centroids do not superimpose well. The same is true for pharmacophore element A in compound **24**. If these elements are not used as fitting points, the RMS is 0.07 Å for both compounds **1** and **24**. In compounds **3, 8** and **9**, the linkers in the body fragments are three carbon atoms long whereas it is two carbon atoms long in the template. The rings superimpose onto the template in a coplanar orientation, but the centroids do not superimpose well. Compound **18** is different from the rest of the compounds, as there is no flexibility in the scaffold holding elements A and B. Elements B and D superimpose well onto the template whereas elements A and C overlay partly. In summary, the compounds described in this section fit the model, but RMS may not be the best parameter to apply in the evaluation of all the fits [29].

Figure 8 shows a superimposition of nine structurally diverse compounds (listed in the Figure text) with pharmacophore element C in the equatorial position relative to the template. Even though the dummy atoms of the interaction point vectors were not used as fitting points, they all fall into the same area.

Using the MMFFs force field, it was not possible to find a low energy conformation of compounds **8, 13** and **14** that fitted the pharmacophore model with pharmacophore element C in the 'equatorial' position (Figure 7, Table 1). Furthermore, compound **6** was found to have an unrealistically large negative

conformational energy (Table 1). To investigate this, conformational analysis of compounds **6, 8** and **13** was repeated with the AMBER* and MM3* force fields. As no MM3* parameters are available for the sulfonamide of compound **14**, the AMBER* and MM2* force fields was used for this structure. Compounds **6, 8, 13** and **14** fitted to the 'equatorial' pharmacophore model were again partially optimised using flat bottom cartesian constrains and AMBER* or MM3* (MM2*) force fields, and their conformational energies were calculated (Table 3). To determine the AMBER* and MM3* (MM2*) global energy minima, conformational searches using the above mentioned force fields were also performed. Compound **8** was found to have a reasonable conformational energy using AMBER* and MM3*. MMFFs seems to overestimate the electrostatic interaction of the 1,3-dihydro-benzoimidazol-2-one oxygen and the protonated amine, whereas AMBER* and MM3* calculates a more reasonable interaction energy. Compound **6** was found to have a high conformational energy penalty using AMBER*, but a negative energy penalty using MM3*. The reason for this force field dependence probably lies in the implementation of the GB/SA solvation model. The solvation energy of 6 is found to be −232 kJ/mol, −323 kJ/mol and −345 kJ/mol by AMBER*, MM3* and MMFFs, respectively.

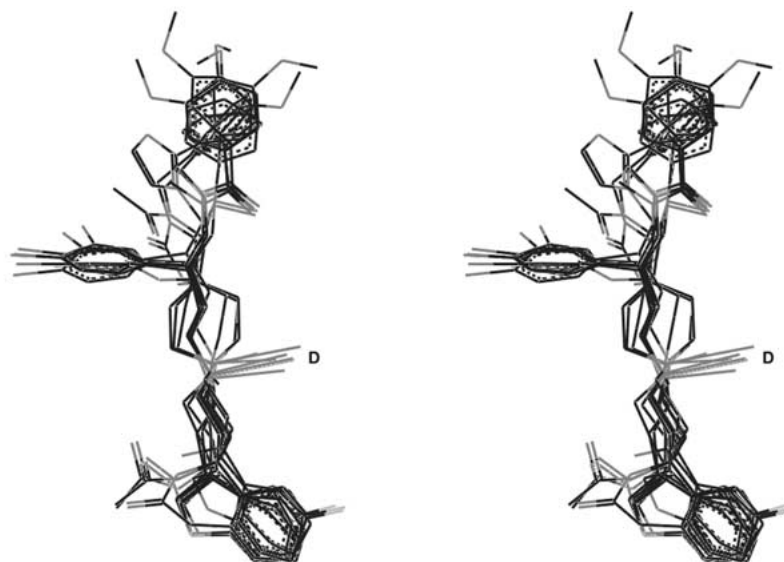The conformational energy penalties of compounds **13** and **14** are found to be high by all

Figure 8. Stereo image. A superimposition of **(S)-2, 3, 4, 6, 10, (R)-11, 12, 19** and **21**. Hydrogens are removed for clarity. Notice how well the interaction point vectors (D) superimpose although they are not used as fitting points.

Table 3. Conformational energy penalties (E_{Conf}/kJ/mol) calculated by various force fields.

Compound	E_{Conf}/AMBER*	E_{Conf}/MM3*	E_{Conf}/MMFFs
6	75.3	−25.4	−63.4
8	−3.4	1.3	35.2
13	103.7	44.3	118.9
14[a]	78.0	87.7	31.8

[a]MM2* data (MM3* parameters of sulfonamide not available).

force fields, but they vary considerably (Table 3). Figure 9 shows the global energy minima of compound **13** found by the use of MMFFs, MM3* and AMBER* compared to the putative bioactive conformation. There is a large difference between these conformations. In the global energy minimum conformation found by AMBER*, all three aromatic rings are stacked, whereas with MMFFs and MM3*, the global energy minima conformations only display stacking of the di-meta-trifluoromethylphenyl and the indole rings. The AMBER* global energy minimum conformation have the di-meta-trifluoromethylphenyl ring sandwiched between the other two rings, whereas in the MMFFs and MM3* global energy minima conformations, the indole lies between the other rings. The MM3* global energy minimum conformation have a hydrogen bond between the protonated amine and the oxygen of the urea group. In the MMFFs global energy minimum conformation and the putative bioactive conformation, a hydrogen bond between the protonated amine and the oxygen of methoxy group is found. The AMBER* global energy minimum conformation has no hydrogen bonds. The stacking of the aromatic rings is probably due to the force fields' inability to correctly calculate the electrostatic attraction between aromatic systems with electron withdrawing and donating substituents. Furthermore, the solvation model might force the compound to adopt a conformation with a small surface area. We suggest that the inability to find a low energy conformation of compound **13** that fit the pharmacophore model is due to these factors.

Figure 10 shows the global energy minima of compound **14** found by MMFFs, MM2* and AMBER* compared to the putative bioactive conformation. In all three global energy minima, there is a hydrogen bond between the protonated nitrogen and the carbonyl in the 2-position of the piperidine-2,6-dione. This hy-
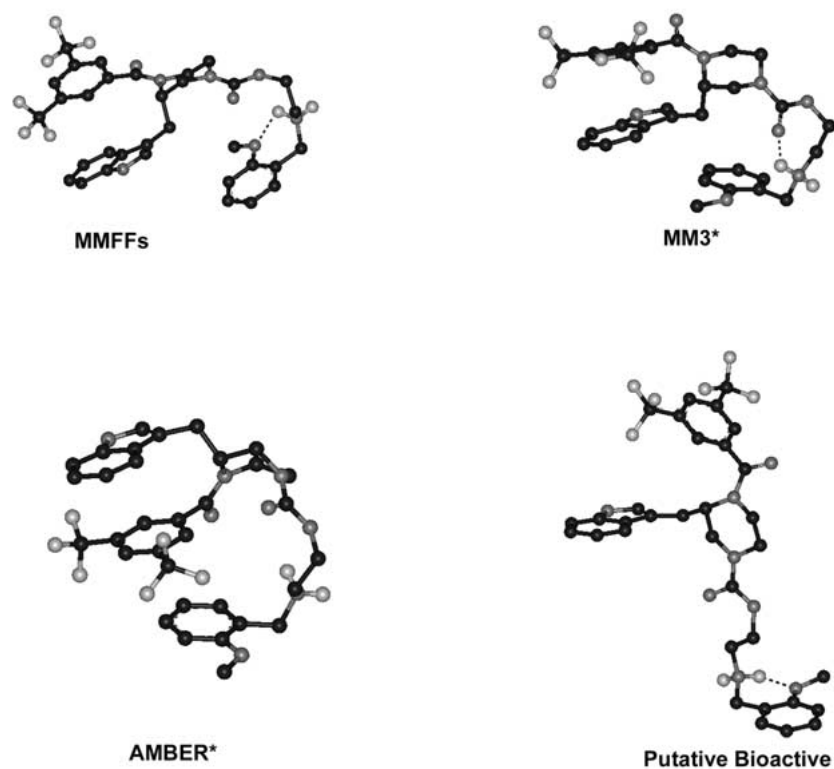
Figure 9. The global energy minima of **13** found by MMFFs, MM3* and AMBER* compared to the putative bioactive conformation. Internal hydrogen bonds are marked with dashed lines.

drogen bond is not present in the putative bioactive conformation. Compound **15** is a close analogue of **14** with similar affinity towards the NK2 receptor (Table 1). In compound **15**, the carbonyl corresponding to the one in the 2-position of compound **14** is lacking. The global energy minimum conformation of compound **15** does not display an internal hydrogen bond, and **15** could be fitted to the pharmacophore model with a low energy penalty (Table 1). The inability to correctly calculate the conformational energies of compounds **14** and **15** is probably an artefact of the forcefields. The combination of the GB/SA solvation model and the force fields overestimates the strength of internal hydrogen bonds leading to the 'collapsed' conformations displayed in Figure 10.

Enantioselectivity

The R enantiomer of compound **2**, ((R)-**2**) was fitted to the model using Flo99. For both the 'axial' and 'equatorial' models, a conformation that superimposed very

well with the template was found (Figure 11). These conformations were imported into MacroModel and relaxed using flat bottom cartesian constraints and the conformational energy calculated to be 19.3 kJ/mol (equatorial) and 18.1 kJ/mol (axial) above compound (S)-**2** (Table 1).

ΔG, the change in free energy can be described by Equation 1 where R is the gas constant, T the temperature and K the equilibrium binding constant.

$$\Delta G = -RT\ln K \qquad (1)$$

This means that each 5.9 kJ/mol of energy penalty will decrease K_i by a factor of 10. For the equatorial and axial conformation, the calculated energy difference between the (S)- and the (R)-enantiomers in the putative bioactive conformations corresponds to a drop in affinity by a factor of 2100 and 1170, respectively. This agrees well with the factor of 1900 found experimentally.

Compound **25** has a chiral centre at the sulphur atom. The (R)-sulfoxide is found to be about 30 times
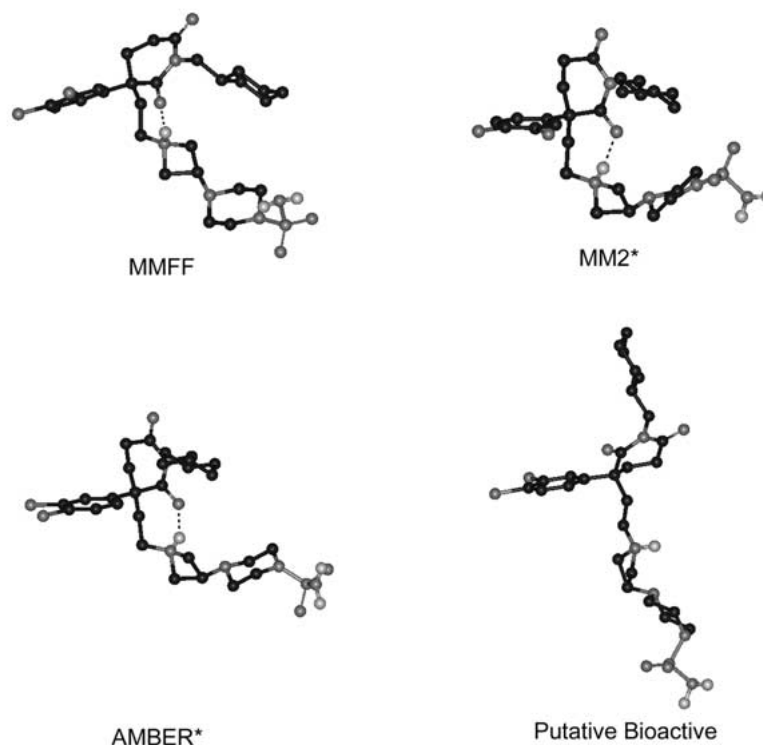
Figure 10. The global energy minima of **14** found by MMFFs, MM2* and AMBER* compared to the putative bioactive conformation. Internal hydrogen bonds are marked with dashed lines.

more active than the corresponding (S)-enantiomer. The formation of an intramolecular hydrogen bond between the hydroxy and sulfoxide groups makes the analysis of the compound difficult. This is not the case for compound **11** where the hydroxy group has been substituted for a methoxy group. Both enantiomers of compound **11** could be fitted to the model. The (R) enantiomer in its bioactive conformation has a conformational energy 6.4 kJ/mol below the (S) enantiomer. If one assumes the same enantioselectivity for compounds **11** and **25**, the conformational energy difference accounts for most of the observed enantioselectivity (a factor of 11). From Figure 12, it is evident that the carbonyl oxygen of (S)-**2** superimposes with the sulfoxide oxygen of (R)-**11** but not that of (S)-**11**. It can also be seen in Figure 8 that several compounds have a carbonyl oxygen that falls within this area. Although a bit speculative, it is tempting to conclude that these oxygen atoms participate in an interaction with the receptor. In that case, another site-point could be defined as a fifth pharmacophore element.
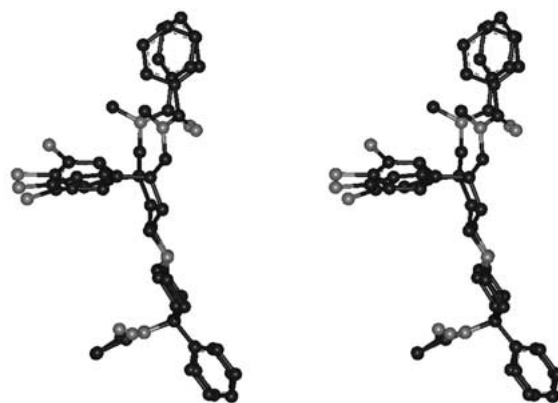

Figure 11. The putative bioactive conformation of (R)-**2** fitted to (S)-**2** (RMS 0.37 Å). Hydrogens are removed for clarity. Both (R)-**2** and (S)-**2** are shown with pharmacophore element C equatorial on the piperidine ring.

Conclusions

A pharmacophore model for NK2 antagonists has been derived. The model consists of three hydropho-
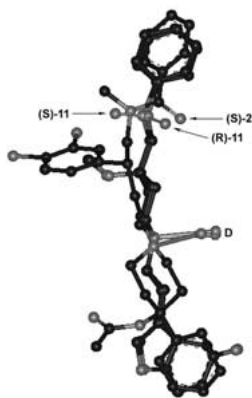
Figure 12. Superimposition of **(R)-11, (S)-11** and **(S)-2**. Hydrogens are removed for clarity. Notice how well the dummy atoms superimpose (D), and the carbonyl oxygen of **(S)-2** and the sulfoxide oxygen of **(R)-11** fall within the same area. This is not true for **(S)-11**.

bic pharmacophore elements (A, B and C) and one hydrogen bond donor acceptor interaction represented as a vector (D). The antagonists bind in an extended conformation with pharmacophore elements A and B in a parallel displaced and tilted arrangement. Relative to the template ((S)-**2**), the pharmacophore element C can be in either an equatorial or an axial conformation, with the former as the most probable. The model was evaluated against 20 structurally diverse, high affinity NK2 and dual NK1 and NK2 antagonists. For all compounds except two, a low energy conformation was found that fitted the model. In these, the hydrogen bond donor was pointing in the same direction. The structures for which no low energy conformation was found had a collapsed global energy minimum. The model was successfully able to explain the stereoselectivities of compounds **2** and **11**.

Acknowledgements

References

1. Regioli, D., Boudon, A. and Fauchére, J.-L., Pharmacol. Rev., 46 (1994) 551.
2. File, S.E., Pharmacol., Biochem. Behav., 58 (1997) 747.
3. Nutt, D., Lancet, 352 (1998) 1644.
4. Raffa, R.B., Neurosci. Behav. Rev., 22 (1998) 789.
5. Schoor, J.V., Joos, G.F., Chasson, B.L., Brouard, R.J. and Pauwels, R.A., Eur. Respir. J., 12 (1998).
6. Sakurada, T., Sakurada, C., Tan-No, K. and Kisara, K., CNS Drugs, 28 (1999) 1997.
7. Bountra, C., Bunce, K., Dale, T., Gardner, C., Jordan, C., Twissell, D. and Ward, P., Eur. J. Pharmacol., 249 (1993) R3.
8. Sprecher, A.v., Gerspacher, M. and Anderson, G.P., Current Research in Rheumatoid Arthritis, 2 (1998) 49.
9. Lowe, J.A., Drozda, S.E., Snider, R.M., Longo, K.P., Zorn, S.H., Morrone, J., Jackson, E.R., McLean, S., Bryce, D.K., Bordner, J., Nagahisa, A., Kanai, Y., Suga, O. and Megumi, T., J. Med. Chem., 35 (1992) 2591.
10. Gao, Z. and Peet, N.P., Curr. Med. Chem., 6 (1999) 375.
11. Gerspacher, M. and Sprecher, A.v., Drugs of the Future, 24(8) (1999) 883.
12. Desai, M.C., Lefkowitz, S.L., Thadeio, P.F., Longo, K.P. and Snider, R.M., J. Med. Chem., 35 (1992) 4911.
13. Elliott, J.M., Broughton, H., Cascieri, M.A., Chicchi, G., Huscroft, I.T., Kurtz, M., MacLeod, A.M., Sadowski, S. and Stevenson, G.I., Bioorg. Med. Chem. Lett., 8 (1998) 1851.
14. Takeuchi, Y., Shands, E.F.B., Beusen, D.D. and Marshall, G.R., J. Med. Chem., 41 (1998) 3609.
15. Swain, C.J., Seward, E.M., Cascieri, M.A., Fong, T.M., Herbert, R., MacIntyre, D.E., Merchant, K.J., Owen, S.N., Owens, A.P., Sabin, V., Teall, M., VanNiel, M.B., Williams, B.J., Sadowski, S., Strader, C., Ball, R.G. and Baker, R., J. Med. Chem., 38 (1995) 4793.
16. Goldstein, S., Neuwels, M., Moureau, F., Berckmans, D., Lassoie, M.-A., Differding, E., Houssin, R. and Hénichart, J.-P., Lett. Pept. Sci., 2 (1995) 125.
17. Jacoby, E., Boudon, A., Kucharczyk, N., Michel, A. and Fauchere, J.-L., J. Recept. Signal Transduction Res., 17 (1997) 855.
18. Vedani, A., Briem, H., Dobler, M., Dollinger, H. and McMasters, D. R., J. Med. Chem., 43 (2000) 4416.
19. Singh, J. and Thornton, J.M., FEBS, 191 (1985) 2989.
20. Williams, D.E., Acta Crystallographica, A36 (1980) 715.
21. Greenfeder, S., Cheewatrakoolpong, B., Billah, M., Egan, R.W., Keene, E., Murgolo, N.J. and Anthes, J.C., Bioorg. Med. Chem., 7 (1999) 2867.
22. Blaney, F.E., Raveglia, L.F., Artico, M., Cavagnera, S., Dartois, C., Farina, C., Grugni, M., Gagliardi, S., Luttmann, M.A., Martinelli, M., Nadler, G.M.M.G., Parini, C., Petrillo, P., Sarau, H.M., Scheideler, M.A., Hay, D.W.P. and Giardina, G.A.M., J. Med. Chem., 44 (2001) 1675.
23. Macromodel V6.5: Mohamadi, F., Richards, N.G.J., Guida, W.C., Liskamp, R., Lipton, M., Caufield, C., Chang, G., Hendrikson, T. and Still, W.C., J. Comput. Chem., 11 (1990) 440.
24. Chang, G., Guida, W.C. and Still, W.C., J. Am. Chem. Soc., 111 (1989) 4379.
25. Halgren, T.A., J. Comput. Chem., 20 (1999) 720.
26. Halgren, T.A., J. Comput. Chem., 20 (1999) 730.
27. Hasel, T.F., Hendrickson, T.F. and Still, W.C., Tetrahedron Comput. Method., 1 (1988) 103.
28. Still, W.C., Tempczyk, A., Hawley, R.C. and Hendrickson, T., J. Am. Chem. Soc., 112 (1990) 6127.
29. Boström, J., Norrby, P.-O. and Liljefors, T., J. Comput.-Aided Mol. Des., 12 (1998) 383.
30. McMartin, C. and Bohacek, R.S., J. Comput.-Aided Mol. Des., 9 (1995) 237.
31. McMartin, C. and Bohacek, R.S., J. Comput.-Aided Mol. Des., 11 (1997) 333.

286

32. Sjöberg, P., in Waterbeemd, H.v.d., Testa, B. and Folkers, G. (Eds.): Computer-Assisted Lead Finding and Optimization, Verlag Helvetica Chimica Acta, Basel 1997, p 83.

33. Spartan 5.0, Wavefunction, Inc., 18401 Von Karman Ave., Suite 370, Irvine, CA 92612, 1997.

34. Wu, E.S.C., Kover, A. and Semus, S.F., J. Med. Chem., 41 (1998) 4181.

35. Qi, H., Shah, S.K., Cascieri, M.A., Sadowski, S. and Mac-Coss, M., Bioorg. Med. Chem. Lett., 8 (1998) 2259.

36. Edmonds-Alt, X., Proietto, V., Broeck, D.V., Vilain, P., Adve-nier, C., Neliat, G., Fur, G.L. and Brelière, J.-C., Bioorg. Med. Chem. Lett., 3 (1993) 925.

37. Harrison, Korsgaard, M.P.G., Swain, C.J., Cascieri, M.A., Sadowski, S. and Seabrook, G.R., Bioorg. Med. Chem. Lett., 8 (1998) 1343.

38. Nishi, T., Fukazawa, T., Ishibashi, K., Nakajima, K., Sugioka, Y., Iio, Y., Kurata, H., Iyoh, K., Mukaiyama, O., Satoh, Y. and Yamaguchi, T., Bioorg. Med. Chem. Lett., 9 (1999) 875.

39. Schnorrenberg, G., Esser, F., Dollinger, H., Jung, B., Speck, G. and Buerger, E., DE4445939-A1.

40. Selway, C.N. and Terrett, N.K., Bioorg. Med. Chem., 4 (1996) 645.

41. Kubota, H., Kakefuda, A., Nagaoka, H., Yamamoto, O., Ikeda, K., Takeuchi, M., Shibanuma, T. and Isomura, Y., Chem. Pharm. Bull., 46 (1998) 242.

42. Smith, P.W., Cooper, A.W.J., Bell, R., Beresford, I.J.M., Gore, P.M., McElroy, A.B., Pritchard, J.M., Saez, V., Taylor, N.R., Sheldrick, R.L.G. and Ward, P., J. Med. Chem., 38 (1995) 3772.

43. Cooper, A.W.J., Adams, H.S., Bell, R., Gore, P.M., McElroy, A.B., Pritchard, J.M., Smith, P.W. and Ward, P., Bioorg. Med. Chem. Lett., 4 (1994) 1951.

44. Jasseand, D., David, S., Antel, J., Brueckner, R., Eeckhout, C. and Bielenberg, G.-W., EP-899270-A1.

45. MacKenzie, A.R., Marchington, A.P., Meadows, S.D. and Middleton, D.S., EP-791592-A2.

46. Mackenzie, R.R., Marchington, A.P., Middelton, D.S. and Meadows, S.D., WO9727185-A1.

47. Burkholder, T.P., Kudlacz, E.M., Le, T.-B. and Maynard, G.D., US5824690-A.

48. Burkholder, T.P., Maynard, G.D. and Kudlacz, E.M., WO9827086-A1.

49. Giardina, G.A.M., Grugni, M., Graziani, D. and Raveglia, L.F., WO-09852942.

50. Miller, S.C., Jacobs, R.T. and Shenvi, A.B., EP-739891-A2.

51. Monaghan, S.M., Alker, D. and Burns, C.J., WO9857972-A1.

52. McCormick, K.D. and Lupo, A.T., WO-09639383.

53. Shankar, B.B., US5688960-A.

54. Shanker, B.B., WO-09818785.

55. Shenvi, A.B., Jacobs, R.T., Miller, S.C., Macht, C.J. and Veale, C.A., WO-09516682.